Chapter 4

Nanostructured ZnO, Cu_2ZnSnS_4, $Cd_{1-x}Zn_xTe$ Thin Films Obtained by Spray Pyrolysis Method

Oleksandr Dobrozhan, Denys Kurbatov,
Petro Danilchenko and Anatoliy Opanasyuk

Additional information is available at the end of the chapter

http://dx.doi.org/10.5772/intechopen.72988

Abstract

The paper presents the investigation on the influence of substrate temperature T_s and the sprayed initial solution volume V_s on structural, substructural, optical properties, and elemental composition of ZnO and Cu_2ZnSnS_4 (CZTS) films as well as state-of-the-art of studying the $Cd_{1-x}Zn_xTe$ (CZT) films obtained by spray pyrolysis technique. The single-phase nanocrystalline ZnO films with average crystallite size of D_C = 25–270 nm and thickness of d = 0.8–1.2 μm can be deposited at substrate temperatures of T_s > 473 K. The continuous CZTS films with optimal thickness (d = 1.3 μm) for application as absorber layers in solar cells were deposited at the sprayed initial precursor volume of V_s = 5 ml. The increase of the substrate temperature up to 673 K caused the significant improvements in the stoichiometry of ZnO films. The optimal stoichiometry ratio of CZTS films for application in solar cells was obtained at V_s = 3–4 ml. Optical study of ZnO films showed that these films have a high-transmission coefficient values of T = 60–80%. To the best of our knowledge, there is the lack of works devoted to the study of CZT films obtained by spray pyrolysis technique.

Keywords: ZnO, Cu_2ZnSnS_4, $Cd_{1-x}Zn_xTe$, thin films, pulsed spray pyrolysis

1. Introduction

ZnO is an *n*-type direct-gap semiconductor with a wide band gap (E_g = 3.37 eV at T = 300 K) having the highest value of exciton energy (60 meV) among the binary compounds [1]. This material is a perspective for application in microelectronics, nanoelectronics, optoelectronics, sensors, solar cells among others due to its unique physical, electrical, and optical properties, non-toxic nature, and chemical and thermal stability in the ambient

atmosphere [2]. It should be noted that, at present, Ukrainian sector of renewable energy, in particular solar, is developing rapidly. First of all it is made possible, thanks to the government support policy. In turn, it leads to an increased interest in the development of new solar cell designs to create further production of solar modules higher efficiency [3, 4]. Due to the absence of rare and toxic elements in zinc oxide compound and possibility to apply low-cost deposition techniques, this material may be an alternative to the traditional ITO ($(In_2O_3)_{0.9}$-$(SnO_2)_{0.1}$) and FTO (SnO_2:F)) transparent conductive layers in thin-film solar cells (SCs) and another optoelectronic device [5]. Nowadays, the perspective substitution of the traditional Si, CdTe, Cu(In,Ga)$(S,Se)_2$ absorption layers in thin-film SCs is considered Cu_2ZnSnS_4 (CZTS) semiconductor compound which has the optimal optical properties (E_g = 1.5 eV, $\alpha \sim 10^4$–10^5 cm^{-1}) [6].

$Cd_{1-x}Zn_xTe$ (CZT) solid solutions are perspective alternative absorption materials to Cu(In,Ga)$(S,Se)_2$ in the tandem solar cells having the band gap value of E_g = 1.1 eV. The appealing advantage of CZT compound is the variation of band gap by changing the zinc concentration. The optimal CZT solid solution with E_g ~1.7 eV can be obtained at the chemical composition of x ~ 0.2 [7]. To achieve the best working characteristics of devices, ZnO, CZTS, and CZT films must have the single-phase structure with large coherent domain sizes (CDS) L, low levels of microdeformations ε, microstresses σ, dislocation concentrations ρ, and well-controlled elemental composition. Unfortunately, typically these films have a high level of defects and secondary phases with different band gaps worsening the performance of the devices based on them. ZnO and CZT films in solar cells should possess high-transmission coefficients and controlled band gaps. Moreover, in order to improve the structural and optical properties of films for application in the low-cost optoelectronic devices, ZnO, CZTS, and CZT films should be deposited by low-cost, non-vacuum methods with optimized physical and technological deposition conditions.

Among the methods to deposit the ZnO, CZTS, and CZT films, special attention is paid to the spray pyrolysis technique having unique advantages: simplicity, efficiency, and cheapness. This technique provides the non-vacuum deposition of a large-area thin film with well-controlled properties.

It was shown [8, 9] that the greatest influence on physical properties and elemental composition of ZnO film has a substrate temperature T_s, CZTS film—the sprayed initial precursor volume V_s. It should be noted that until now CZT films deposited by spray pyrolysis technique are not well-studied, except some works [10, 11].

Thus, the investigation of the influence of deposition conditions on structural, substructural, and optical properties of ZnO, CZTS, and CZT films deposited by spray pyrolysis technique is the perspective in terms of its application in highly efficient optoelectronic devices.

2. ZnO, CZTS, and CZT thin films deposition methods. Peculiarities of the spray pyrolysis technique

The wide range of methods is well developed to deposit ZnO, CZT, and CZTS films which split into physical (for example, magnetron sputtering [12–14]) and chemical (for example,

spray pyrolysis [5, 8–10]) techniques. Typically, the physical methods allow to obtain more perfect films with a higher structural quality, and these methods provide a precise control of the films thickness and low content of defects in deposited material compare to chemical methods, but physical deposition techniques require the usage of more complicated equipment and presence of high level of vacuum, thus they are energy-consuming. In contrary, chemical techniques to deposit ZnO, CZTS, and CZT films are low-cost and energy savers. Among them, spray pyrolysis method is considered as the most promising technique. This technique is simple and non-vacuum providing the deposition of the continuous, porous, nanostructured films, and multilayered structures [15].

Taking into account the increased interest to the nanosized materials with properties, significantly different to bulk materials (caused by quantum-size effect), several scientific groups have obtained the nanocrystalline ZnO and CZTS films [16, 17]. It is important to note that the works dedicated to the study of the nanosized structures used chemical techniques for films deposition. ZnO, CZTS, and CZT films deposited by spray pyrolysis technique are not yet well-studied; this fact conditioned the aim of our study.

The image of laboratory setup developed for the deposition of ZnO, CZTS, and CZT films by pulsed spray pyrolysis is showed in **Figure 1**. It consists of a spraying gun with initial precursor volume reservoir (1), spraying nozzle (2), and microcontroller block (3), allowing the control of the number of spraying cycles, time, and pauses between cycles. To the spraying gun, the compressor with pressure regulator (4) is connected with the aim of producing the air flow for transportation of the dispersed precursor onto heated substrate surface. Between the spraying gun and the compressor, an electromagnetic valve (5) is installed, where the "open" and "closed" regimes are controlled by the microcontroller block (3). The heating of substrate (6) is provided by the heating plate (7). During the deposition of films by spray pyrolysis technique, the properties of ZnO, CZTS, and CZT condensates are dependent on the precursor choice and physical, chemical deposition conditions. **Table 1** presents the overview of deposition conditions and precursors typically used to deposit the ZnO, CZTS, and CZT films by spray pyrolysis technique.

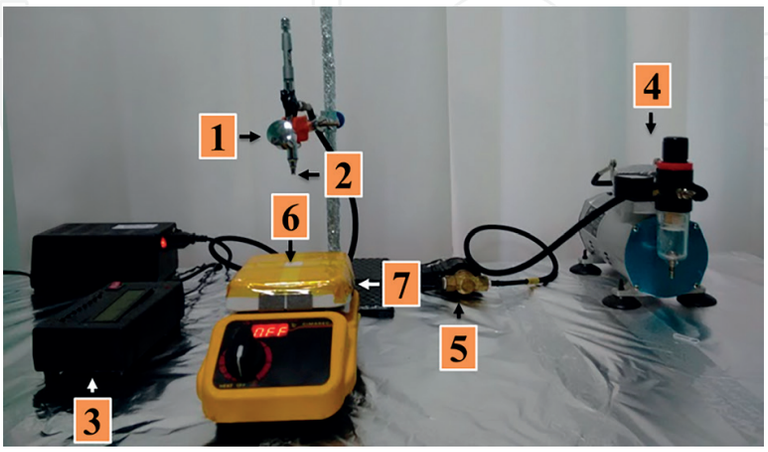

Figure 1. Image of the experimental setup for ZnO, CZTS, and CZT films deposition by pulsed spray pyrolysis: (1) spraying gun with initial precursor volume reservoir, (2) spraying nozzle, (3) microcontroller block, (4) compressor, (5) electromagnetic valve, (6) substrate, and (7) heating plate [18, 19].

№	Initial precursor	Solvent	Concentration (M)	Substrate type	Substrate temperature, T_s (K)	Ref.
ZnO films deposition						
1	Zinc chloride ($ZnCl_2$)	H_2O	0.10	Silicon	623–823	[21]
		H_2O	0.10	Glass	773	[22]
		H_2O	0.10	Glass	523–723	[23]
2	Zinc acetate ($Zn(CH_3COO)_2{\cdot}2H_2O$)	H_2O	0.04	Glass	573	[24]
3	Zinc acetate $Zn(CH_3COO)_2$	$H_2O + CH_3OH$	0.20	Glass	693	[25]
		H_2O	0.50	Glass	453–723	[26]
		H_2O	0.10	Glass	623	[27]
CZT films deposition						
4	Cadmium chloride ($CdCl_2$) Zinc chloride ($ZnCl_2$) Tellurium chloride ($TeCl_4$)	H_2O	0.02 (1:1:3)	Glass	250–325	[10, 11]
CZTS films deposition						
5	Copper chloride ($CuCl_2$) Zinc chloride ($ZnCl_2$) Tin chloride ($SnCl_2$) Thiourea ($CS(NH_2)_2$)	$(CH_3)_2SO$	0.010 0.005 0.005 0.040	Soda-lime glass	623	[28]
6	Copper chloride ($CuCl_2$) Zinc chloride ($ZnCl_2$) Tin chloride ($SnCl_2$) Thiourea ($CS(NH_2)_2$)	$H_2O + C_2H_5OH$	0.020 0.010 0.010 0.080	Soda-lime glass	553–633	[29]

Table 1. Precursors and physical-chemical conditions to deposit the ZnO, CZTS, and CZT films by spray pyrolysis method.

It should be noted that in order to obtain initial molecular solution for the deposition, the typical materials are metal salts dissolved in polar solvents, particularly in water, ethanol, etc. The most common substrates used are the non-oriented glass and silicon slides. The average substrate temperature is in the range of 250–823 K. It should be noted that these values are lower in comparison to the substrate temperatures used in physical methods.

http://dx.doi.org/10.5772/intechopen.72988

3. Morphological, structural, and substructural properties of ZnO and CZTS films obtained by spray pyrolysis technique

The surface morphology, structural, substructural, optical properties, and chemical composition of ZnO and CZTS films deposited by spray pyrolysis method are determined by its physical, chemical, and technological deposition conditions.

3.1. The morphological properties

SEM images of ZnO films deposited at different substrate temperatures are presented in **Figure 2a–d** [19, 20]. It has been shown that at substrate temperatures higher than 473 K, crack-free and continuous nanocrystalline ZnO films with a good adhesion to substrate were formed.

The average grain size in the condensates was in the range of D_C = (25–270) nm (see inset in **Figure 2d**), increasing under the increase the deposition temperature up to 673 K. Whereas, the film thickness determined by the cross-sectional image was d = 0.8–1.2 μm.

One of the main film parameters of CZTS films is its thickness, which is typically controlled by the dispersed precursor volume V_s. Dependence CZTS films properties vs. films thickness in the range of d = 0.244–0.754 μm was studied by authors [9]. These values are not optimal for absorption of nearly 100% solar radiation because of the necessity CZTS films with thickness of d = 1–3 μm [6].

Thus, we have studied the CZTS films deposited by spray pyrolysis technique at different sprayed initial precursor volumes which had the higher thickness than studied in Ref. [9].

In **Figure 2e–h**, the SEM images of CZTS films and its cross-section deposited at different V_s are presented. It can be seen that in the range of studied values continuous films were formed,

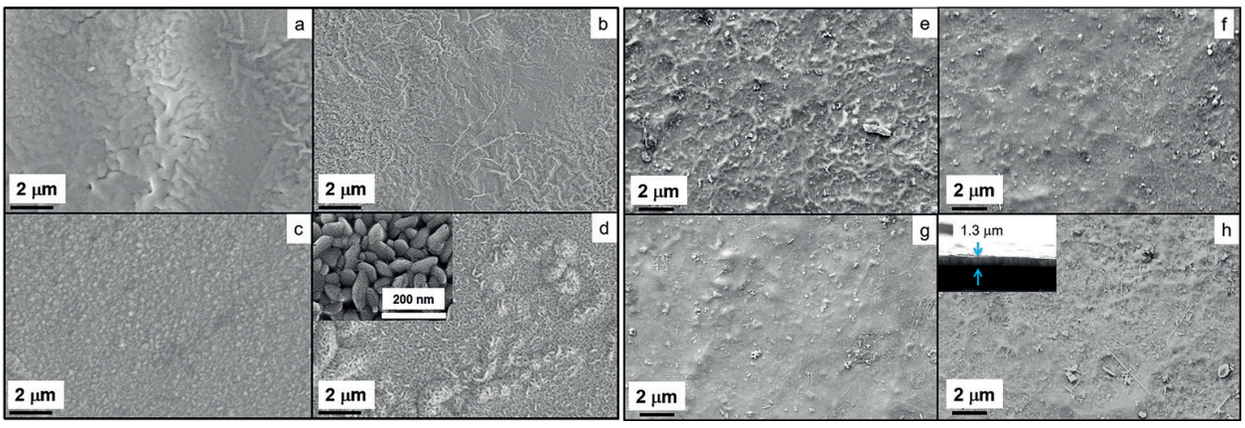

Figure 2. SEM images of ZnO films surface deposited at different temperature T_s, K: 473 (a), 573 (b), 623 (c), and 673 (d). Inset (d) shows the film surface with high resolution obtained at 673 K [19] and CZTS films surface deposited at different dispersed initial precursor volumes V_s, ml: 2 (e), 3 (f), 4 (g), and 5 (h). Inset (h) shows the films' cross-section [20].

which had a well adhesion to substrate and characterized by the absence of cracks and holes on their surfaces. The maximal layer thickness is determined by the cross-section method and it was d = 1.3 μm at V_s = 5 ml (**Figure 2h**).

3.2. Structural and substructural properties

Structural and substructural properties of ZnO and CZTS films have a significant influence on functional characteristics of devices [18–20]. Thus, its study is an important scientific objective. For example, band gap of zinc oxide films can be significantly increased by means of nanostructuring due to the quantum-size effects. At the same time, CZTS films as the absorber layers is SC should have the crystallites with sizes larger that diffusion length of minority charge carriers [6]. However, the films obtained by spray pyrolysis are usually characterized by high levels of microdeformations, microstresses, and density of dislocations in comparison to the values observed in the condensates deposited by physical vacuum methods, e.g., thermal evaporation, magnetron sputtering, etc.

The detailed description of methods applied to study structural, substructural, and optical properties of films is described elsewhere [18–20].

In **Figure 3a**, the XRD patterns of ZnO films deposited at different substrate temperatures are presented. On the diffraction patterns of the low-temperature films is dominated the diffraction line at angles 35.60–36.10° that corresponds to the reflection from (101) plane of ZnO hexagonal phase. On the diffraction patterns of the films deposited at T_s > 573 K, the lines at angles 31.80° and 34.80° are dominated, which correspond to the reflections of (100) and (002) crystallographic planes, respectively. X-ray analysis has been shown that deposited samples are single-phase and contain ZnO hexagonal phase. Secondary phases have not been determined by XRD analysis.

In **Figure 3b**, the X-ray patterns of CZTS films deposited at different dispersed solution volumes are shown. As can be seen from **Figure 3b**, on X-ray patterns is dominated the line on angles 28.05–28.50° which corresponds to the reflection from (112) CZTS tetragonal phase

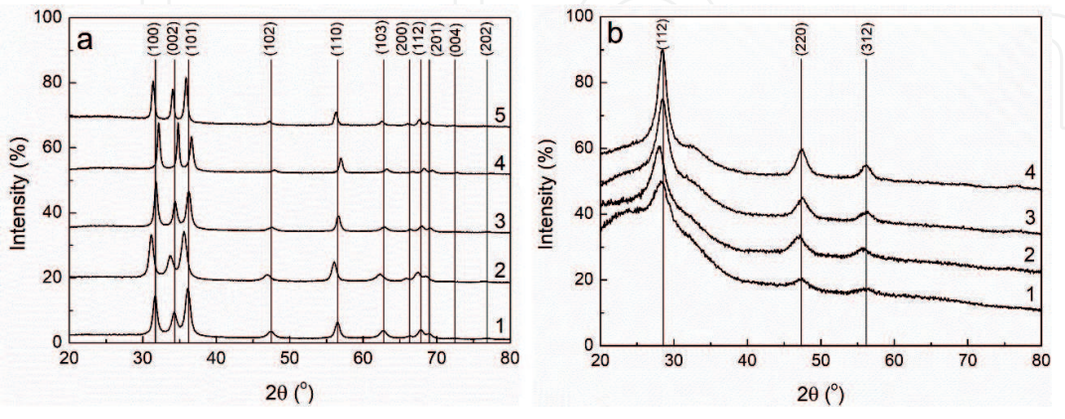

Figure 3. XRD patterns of ZnO films obtained at different substrate temperatures T_s, K: 473 (1), 523 (2), 573 (3), 623 (4), and 673 (5) (a); and CZTS films deposited at different dispersion solution volume V_s, ml: 2 (1), 3 (2), 4 (3), and 5 (4) (b). Vertical lines correspond to the JCPDS cards (ZnO— № 01–089-1397; CZTS— № 00–026-0575) [19, 20].

crystallographic plane. There are also presented lines at angles 47.15–47.50° and 55.55–56.45° which correspond to the reflection from (220) and (312) CZTS planes, respectively. It should be noted that during the increasing of precursor volume the intensity of peaks is increased and its half-width is decreased. It may be caused by the increasing of film thickness and by improvement of the films' crystalline quality. It is well-known that intensities ratio between the number of diffraction reflections from kesterite and stannite crystallographic planes is different [30]. Taking into account this fact, determination of these ratios gives an opportunity to estimate precisely the materials dominate phase. The measured intensity ratio $I_{(112)}/I_{(220)}$ from (112) and (220) crystallographic planes films was 2.23–2.56. These values are similar to the values, determined for un-doped films with kesterite phase ($I_{(112)}/I_{(220)} \approx 2.80$) [31]; thus, most probably, the investigated films have a kesterite phase. This conclusion is confirmed by the experimental measurements of lattice constants ratio ($c/2a$ = 0.9970–1.0203), that was similar to 1.0. These values are typical for kesterite [32].

Lattice parameter of the materials is a characteristic which is very sensitive to stoichiometry varying, impurities introduction, oxidation, etc. Thus, the precise determination of these values allows us to study the corresponding processes.

In **Figure 4**, the dependencies of ZnO and CZTS films lattice parameters a, c vs. deposition conditions are presented. In **Figure 4a**, it can be seen that during the increase of substrate temperature, measured parameters a, c for ZnO films are approached to the reference data that may be caused by the film stoichiometry improvement. High-temperature condensates composition approaching to the stoichiometric is confirmed by the chemical composition analysis data. In case of CZTS films (**Figure 4b**) most similar to the reference data a and c values are obtained by us at V_s = 4–5 ml, that is well-correlated with elemental composition analysis. It was estimated that lattice parameters are varied in the range of a_{ZnO} = 0.32477–0.32554 nm, c_{ZnO} = 0.51507–0.52111 nm, c/a_{ZnO} = 1.5822–1.6046, a_{CZTS} = 0.5423–0.5480 nm, c_{CZTS} = 1.0823–1.1182 nm, and $c/2a_{CZTS}$ = 0.9970–1.0203, the unit cell volume was in the range of $V_{cell(ZnO)}$ = 0.0427–0.0477 nm^3 and $V_{cell(CZTS)}$ = 0.3183–0.3358 nm^3, that is well-correlated to the reference data [31] and values obtained for ZnO and CZTS films deposited by spray pyrolysis technique in Ref. [34].

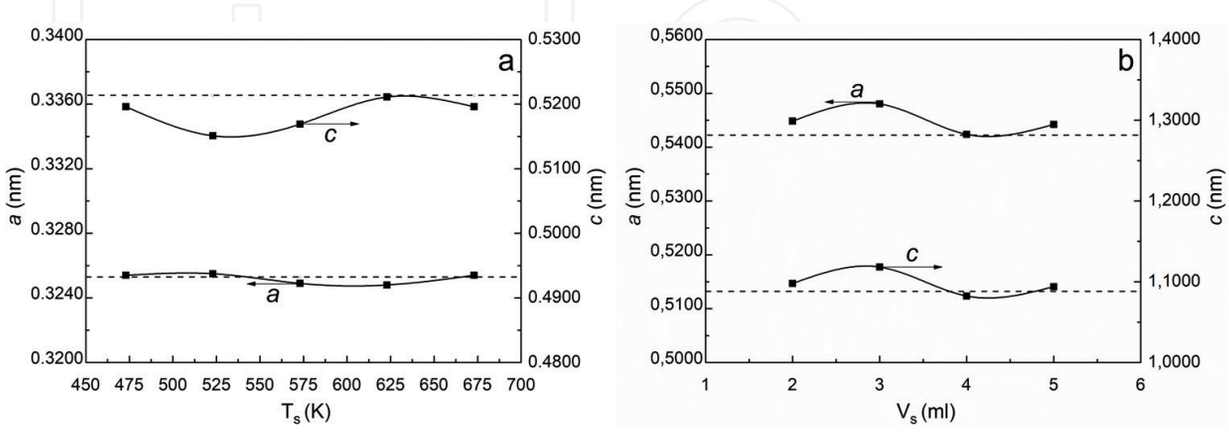

Figure 4. The dependencies of the lattice parameters a, c on the physical and technological deposition conditions [substrate temperature T_s, K—for ZnO films (a) dispersion solution volume V_s, ml—for CZTS films (b)]. Horizontal lines are corresponding to the stoichiometric material.

In **Figure 5**, the results of measurements L and ε parameters in studied films by threefold convolution method are presented. As can be seen from **Figure 5a**, in ZnO films during the increasing of substrate temperature from 473 to 673 K, there is a tendency of the CDS values increasing in direction of [100]—from L ~ 14 to ~ 21 nm, in direction of [101]—from L ~ 11 to ~ 20 nm and in direction of [102]—from L ~ 10 to ~ 63 nm. Similar L-T_s dependencies are observed in our previous works [33], where II-VI type compounds (CdTe, ZnS, ZnSe, and ZnTe) were obtained by close-spaced vacuum sublimation technique. At the same time, the microdeformations level in ZnO films in direction of [100] is decreased from $\varepsilon \sim 1.6 \times 10^{-5}$ to ~ 0.5×10^{-5}, in direction of [101]—from $\varepsilon \sim 3.5 \times 10^{-5}$ to ~ 1.2×10^{-5}, in direction of [102]—from $\varepsilon \sim 1.0 \times 10^{-5}$ to ~ 0.7×10^{-5}, at the same substrate temperatures range (**Figure 5b**). Similar ε decreasing at substrate temperatures of $T_s > 573$ K is observed in CdTe and ZnTe films [35].

As can be seen from **Figure 5c**, in CZTS films during the increasing of the dispersion solution volume from 2 to 5 ml, CDS values are almost were not changed: L ~ 24–26 nm (for (112)–(220) planes pair), L ~ 25–27 nm (for(112)–(312) planes pair), and L ~ 39–40 nm (for (220)–(312) planes pair). Consequently, V_s varying influence on CDS sizes is negligible. It should be noted that obtained results of L measurements are well-correlated to the results presented in Refs. [36], where CZTS films were deposited under the similar experimental conditions. At the

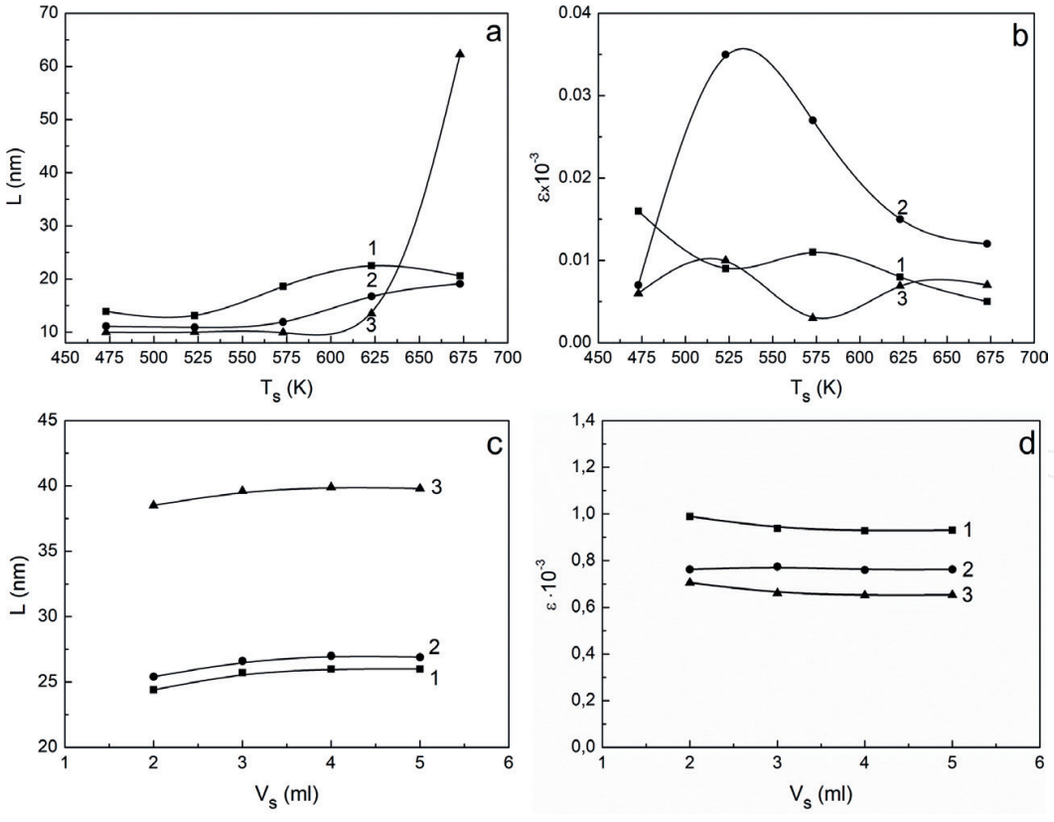

Figure 5. Influence of the substrate temperature on CDS values (a) and microdeformations level (b) of ZnO films on direction normal to the (100)–(200) (1), (101)–(202) (2), (102)–(103) (3) crystallographic planes and of the dispersion solution volume V_s on L (c) and ε (d) for CZTS films on direction normal to the (112)–(220) (1), (112)–(312) (2), (220)–(312) (3) planes. The threefold convolution technique was used.

same time, the microdeformations level in CZTS films for the directions normal to (112)–(220) crystallographic planes is varied in the range of $\varepsilon \sim (0.93–0.99) \times 10^{-3}$; for (112)–(312) planes—$\varepsilon \sim (0.76–0.77) \times 10^{-3}$; for (220)–(312) planes—$\varepsilon \sim (0.65–0.71) \times 10^{-3}$ (**Figure 5d**). It should be noted that measured microdeformations values in CZTS films are lower than presented in Ref. [37], where $\varepsilon \sim (1.26–6.60) \times 10^{-3}$. The measured level of microdeformations allowed us to determine the level of microstresses (σ) in nanocrystalline ZnO and CZTS films. It was estimated that microstresses levels in ZnO and CZTS films varied in the ranges of σ_{ZnO} = 0.48–1.53 MPa, σ_{CZTS} = 5.2–20.3 MPa, respectively. The influence of T_s onto σ level in ZnO films was also studied in Refs. [8], where authors estimated that during the increase of T_s from 623 to 723 K the compression stress level σ was decreased (1.77–1.47 GPa).

In CZTS films, during the increase of the dispersion solution volume microstresses level is decreased, wherein the smallest σ values are observed in layers obtained at V_s = 5 ml.

In **Figure 6**, the results of measurements of the dislocations concentration on the boundaries (ρ_L) and within volume (ρ_ε) CSDs blocks and of the general dislocations concentration (ρ) in direction normal to (100) crystallographic plane for ZnO films or (112) crystallographic plane for CZTS films are presented. Studied ZnO layers are characterized by rather low values of $\rho = (1.3–6.1) \times 10^{13}$ lines/m^2 compare to the results obtained by other authors. As it can be seen from **Figure 6a**, during the increase of T_s, there is a tendency to decrease ρ values. In Ref. [38], authors have estimated that in ZnO nanocrystalline films with thickness of d = 0.135–0.392 μm, deposited at T_s = 473 K, the dislocation concentration values are higher ($\rho = (1.29–4.15) \times 10^{15}$ lines/m^2) than determined here. In Ref. [39], authors have also obtained higher values ($\rho = (2.4–5.8) \times 10^{13}$ lines/m^2) compared to our results. It has been shown that during the increase of V_s (**Figure 6b**) in CZTS films general dislocation density ρ does not almost change in all investigated directions.

The smallest values of $\rho = (17.0–19.3) \times 10^{15}$ lines/m^2 are obtained in case of film deposited at dispersion volume of V_s = 5 ml. It should be noted that these values ρ are smaller than observed earlier for CZTS films deposited by chemical methods (spray pyrolysis – $\rho = (11.6–80.3) \times 10^{16}$ lines/m^2) [35]), and higher compare to the films obtained by vacuum methods (thermal evaporation – $\rho = (0.64–4.00) \times 10^{14}$ lines/m^2 [40]).

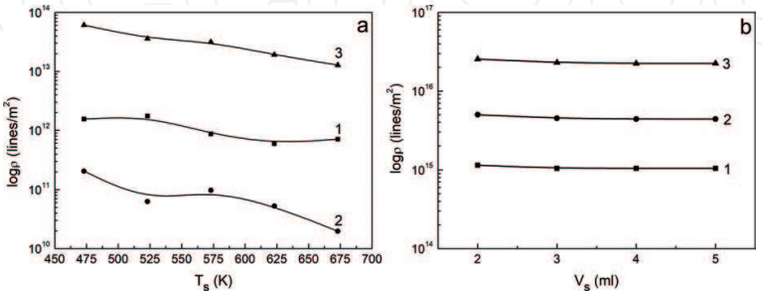

Figure 6. The influence of substrate temperature T_s (in case of ZnO films (a)) and dispersed initial solution volume V_s (in case of CZTS films (b)) on dislocations density ρ: on the sub-grain boundaries (1), within CDS units (2) and general dislocations concentration (3) for the direction normal to (100)–(200) planes for ZnO and to (112)–(220) planes for CZTS. The measurements error was varied in the range of 15–20%.

3.3. The study of the stoichiometry

Energy dispersed analysis of the X-ray spectra (EDAX) allows us to determine the elemental composition of ZnO and CZTS films obtained in present work. Results determined for films deposited at different physical-chemical and technological conditions are presented in **Table 2**. As it can be seen, ZnO films have some oxygen surplus on zinc. Besides, films stoichiometry is increased during the increasing of the substrate temperature. This fact is confirmed by the concentration ratios C_O/C_{Zn}, that are parts of compound (γ_{ZnO} = 1.4 – T_s = 473 K, γ_{ZnO} = 1.2 – T_s = 623 K). The impurities connected to the films contamination by the precursor materials have not been determined.

The control of CZTS films elemental composition is a complex and important task because of its probable determination of the phase conditions, crystal structure, optical, and electrical properties of investigated layers. It was estimated that in CZTS films some copper, zinc, and tin are present in surplus and has some sulfur deficiency. Sulfur losses in films during the pyrolytic reaction of the initial precursor near the surface of the heated substrate may be caused by its high volatility [41]. It should be noted that stoichiometry of studied films is some improved during the increasing of dispersed precursor volume. Also, the obtained ratio γ_{CZTS_1} = (0.80–0.84) in CZTS films deposited at precursor dispersion with volume of V_s = 2–3 ml is close to the optimal values necessary to develop SCs with high solar energy conversion efficiency (γ_{CZTS_1} = (0.8–0.9), γ_{CZTS_2} = (1.1–1.2)) [40, 42]. For film obtained by dispersion precursor volume of 3 ml for this requirement corresponds the next ratio—γ_{CZTS_2} = 1.2. Impurities related to the films' contamination by the precursor's materials have also not been observed in CZTS layers.

ZnO							
T_s **(K)**	C_{Zn} **(at. %)**	C_O **(at. %)**			γ_{ZnO}		
473	41.8	58.2			1.4		
523	42.3	57.7			1.4		
573	42.6	57.4			1.3		
623	44.3	55.7			1.2		
673	44.0	56.0			1.2		
Stoichiometry	50.0	50.0			1.0		
CZTS							
V_s (ml)	C_{Cu} (at. %)	C_{Zn} (at. %)	C_{Sn} (at. %)	C_S (at. %)	γ_{CZTS_1}	γ_{CZTS_2}	γ_{CZTS_3}
2	28.6	21.4	14.3	35.8	0.8	1.5	0.8
3	27.0	17.3	14.7	40.8	0.8	1.2	0.7
4	27.7	16.3	15.1	40.9	0.9	1.0	0.6
5	26.4	15.2	15.4	43.0	0.9	1.0	0.6
Stoichiometry	25.0	12.5	12.5	50.0	1.0	1.0	0.5

Table 2. Measurement results of the chemical composition for ZnO and CZTS films obtained at different conditions.

http://dx.doi.org/10.5772/intechopen.72988

4. Optical properties of ZnO and CZTS films obtained by spray pyrolysis technique

4.1. Optical properties

The study and control of the optical properties of ZnO, CZTS, and CZT films is an important task with the aim of their usage in optoelectronic devices, especially for SCs development. It is well-known that optical characteristics of these films heavily dependent on morphological, structural, substructural properties, chemical composition, and physical (chemical) and technological deposition conditions.

In present work, the transmission light coefficient of ZnO films was in the range of T = 60–80% at the wavelength range of λ = 430–800 nm. The highest transmission values had films obtained at T_s = 673 K. It was estimated that measurement E_g values for ZnO films were in the range of 3.18–3.30 eV and were also dependent on T_s.

As can be seen from **Figure 7a**, band gap E_g of zinc oxide during the increasing of the deposition temperature is at first increased and in further decreased. This complex dependence of E_g may be caused by increasing of the grain sizes in films and by improvement of their structural quality during the increasing of T_s. It is well known [43] that in nanocrystalline films (D_C < 100 nm) band gap is determined by quantum effects, that leads to the increasing of E_g compare to the values observed in bulk materials. During the increasing of the grain size, quantum effects are gradually decreased. At the same time, due to the high level of the substructural defects (primarily dislocations) in nanocrystalline films, that have been given the local deformations on the materials lattice, its average E_g have been smaller than in bulk materials [16]. At high substrate temperatures, films with sufficient large grain size and low structural defect concentration were formed. As a result, the band gap of semiconductor is approaching the bulk value. Similar tendencies of E_g changing depending on the deposition temperature were observed in Refs. [44].

In **Figure 7b**, dependence of the materials E_g on the dispersed solution precursor volume V_s is presented. It should be noted that the smallest α values have been obtained for layers

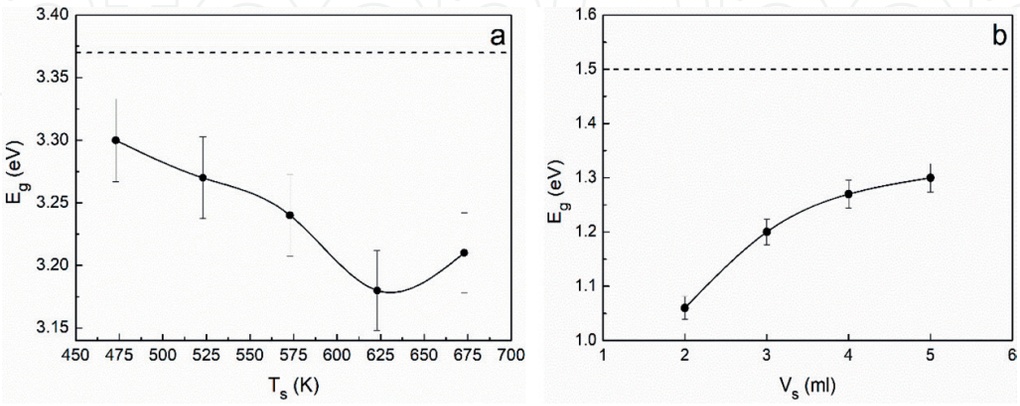

Figure 7. Bang gap (E_g) dependencies on substrate temperature T_s in ZnO films (a) and on dispersion solution volume V_s in CZTS films (b). Dashed line corresponds to band gap value in bulk ZnO (E_g = 3.37 eV) and bulk CZTS (E_g = 1.50 eV).

deposited at volume of V_s = 2 ml, the highest values—at V_s = 5 ml, respectively. It is quite typical because of the smallest and highest thickness values of the corresponding layers. During the increasing of dispersed initial precursor solution volume, the values of band gap were varied in the range of E_g = 1.06–1.30 eV and were approximately approached to the values typical for bulk stoichiometric material (E_g = 1.5 eV). It indicates on increasing of grain sizes and decreasing of films deficiency during the increasing of their thickness. Similar tendencies have been observed in Ref. [9].

4.2. Raman and Fourier transform IR (FTIR) spectra

Raman spectroscopy is an additional to X-ray diffraction analysis method of studying the phase composition and quality of ZnO, CZTS, and CZT thin films.

Raman spectra of ZnO films measured in the range of frequencies 90–800 cm^{-1} are presented in **Figure 8a**. In spectra, a number of different intensity lines on the next frequencies: 95–98, 333–336, 415, 439–442, 572, and 578–587 cm^{-1} are observed. Using the reference data, these lines were interpreted by us as the next phonon modes: $E_2^{low}(Zn)$ [43–45], E_2^{high}-E_2^{low} [46], $E_1(TO)$ [45], $E_2^{high}(O)$ [43–47], $A_1(LO)$ [43] and $E_1(LO)$ [45–46]. In **Figure 8a**, two intensive peaks, which correspond to E_2 mode, are also observed: peak E_2^{high}, which is relative to the oxygen anions, is localized at frequency of 439–442 cm^{-1} and peak E_2^{low}, which is relative to zinc cations, is localized at frequency of 95–98 cm^{-1}. It is well known [49] that the crystalline quality of ZnO films has a direct influence on the mode E_2 intensity. Besides, $E_2^{high}(O)$ peak is very sensitive to the presence of inner defects of material. The deviation of the frequency $E_2^{high}(O)$ peak from the value typical for bulk ZnO (437 cm^{-1}), that is observed by us in low-temperature condensates, indicates about the presence in zinc oxide high level of microstresses and stretched defects (dislocations) density of the lattice. It should be noted that during the increase of the substrate temperature, the $E_2^{high}(O)$ peak position is some red-shifted from 442 cm^{-1} to the typical bulk ZnO values—439 cm^{-1}, which indicates the decrease of σ and ρ levels.

FTIR spectroscopy is an addition to X-ray diffraction analysis and Raman spectroscopy technique, which allows to obtain an information about the elemental composition of the studied material and its contamination by the precursor impurities. The number of frequencies,

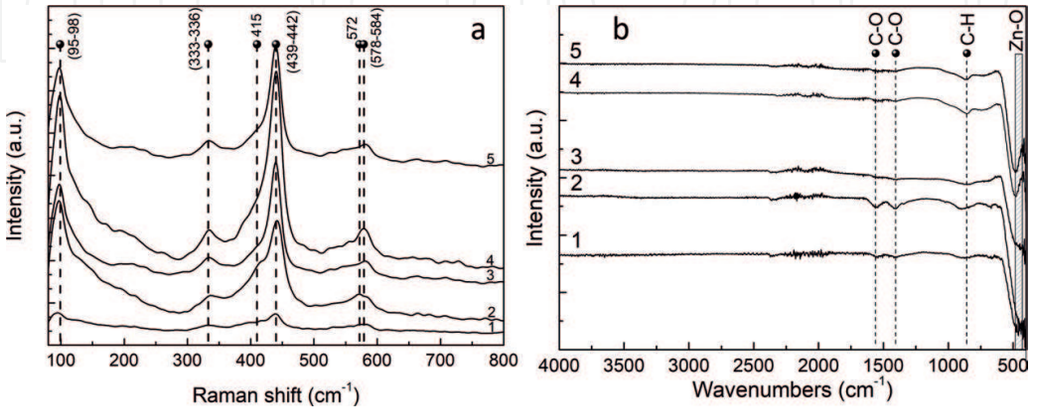

Figure 8. Raman (a) and FTIR (b) spectra of ZnO films deposited at different substrate temperatures T_s, *K*: 473 (1), 523 (2), 573 (3), 623 (4), and 673 (5).

http://dx.doi.org/10.5772/intechopen.72988

where the light absorption and transmission in films are performed, allows us to determine the functional links between chemical elements which are part of the studied materials.

In **Figure 8b**, FTIR reflection spectra of ZnO films deposited at different substrate temperatures are presented. Although that thin films were deposited in air by chemical technique obtained spectra were comparatively pure.

At low frequencies (460–475 cm^{-1}), there is observed minima, which due to the reference data [48], correspond to Zn-O vibrational mode. It should be noted that FTIR spectra obtained on films deposited in all range of substrate temperatures have a C-Cl vibrational mode [50]. The presence of this connection may be caused by the usage of HCl acid, which was added as a precursor during its preparation. The acid paths are also observed in films. In FTIR spectra of ZnO films deposited at $T_s < 573$ K, peaks on the frequencies 1405 and 1560 cm^{-1} are presented; they were interpreted by us as symmetric and asymmetric C-O vibrational modes [50]. The absence of C-O connections in films deposited at $T_s > 573$ K indicates about the total precursor decomposition near the substrate surface at these temperatures. It eliminates the possibility of adsorption of the acetate elements on ZnO films surface during the pyrolysis, and it leads to the formation of single-phase zinc oxide polycrystalline films.

It is well known that in CZTS films, the presence of secondary phases, such as Cu_xS_y, Zn_xS_y, Sn_xS_y, Cu_xSnS_y, ZnO, and Zn_xSnO_y, is available [39, 51–53]. They are characterized by affiliated lattices, and they indicate on XRD patterns refractions on similar angles. It complicates the phase analysis by XRD technique. Thus, for precise identification of the secondary phases in CZTS compound, the researchers often use Raman spectroscopy in addition to XRD analysis [54]. It allows to identify not only secondary phases, but also kesterite and stannite. In **Table 3**,

Experimental data				**Literature data**			
V_s, ml				Raman shift, cm^{-1}	Symmetry	Mode	Reference
2	3	4	5				
Raman shift (cm^{-1})							
Green-laser (λ = 514.5 nm)							
142				143–144	E	*CZTS E*	[56]
340				338–339	A	*CZTS A*	[54]
664				672	A	*2a CZTS A*	[56]
Red laser (λ = 632.8 nm)							
339				338–339	A	*CZTS A*	[52]
663				672	A	*2a CZTS A*	[57]
UV-laser (λ = 325 nm)							
340				341	A	*CZTS A*	[56]
—	560	—	—	541	—	*ZnO*	[45]
664				672	A	*2a CZTS A*	[57]

Table 3. Peaks interpretation presented on Raman spectra of CZTS films.

the results of study the Raman spectra of CZTS films using as an excitation source the radiation of several lasers are presented. At all spectra regardless on the precursor volume and excitation laser type, the main peak on frequencies of (339–340) cm^{-1} is presented. It is well correlated to the results of previous studies [52, 54, 55]. In Raman spectra obtained using the green laser, lines on the next frequencies: 142, 340, and 664 cm^{-1} are also observed, which correspond to *CZTS E*, *CZTS A*, and *2a CZTS A* (*CZTS A* mode phonon replica) phonon modes, respectively [54–56].

Usage of the red- and UV-lasers as phonons excitation source allows us to increase the method's sensitivity onto the revealing of compounds with optical band gap close to E_g ~ 1.96 and ~ 3.81 eV (excitation radiations energies of corresponding lasers). On spectra, obtained using the red- and UV-lasers, are presented lines on frequencies 339–340 cm^{-1}, 663–664 cm^{-1} which correspond to the *CZTS A* and *2a CZTS A* phonon modes [52, 56, 57]. The usage of UV-laser in one of the studied films revealed a negligible number of ZnO secondary phase. In addition, these results are supported by the phonon excitation in Raman spectra on the frequency at 560 cm^{-1} on film obtained from the precursor volume dispersion of 3 ml. Other secondary phases in studied films are not revealed. Raman spectra of CZT films measured during the influence of green-laser excitation radiation (λ = 514 nm, E = 2.41 eV) are presented in **Figure 9**. In the spectra of the CZT sample (x = 0.32), peak which corresponds to LO_2(ZnTe) mode is observed. In these spectra, intensive peaks which correspond to A_1(Te) E_{TO}(Te) telluric modes are also detected. In the spectra of the CZT sample (x = 0.75), is observed a weak peak that corresponds to A_1(Te) mode, peaks of the next modes: LO_1(CdTe), TO_1(CdTe), TO_2(ZnTe), LO_2(ZnTe), and also detected the LO_2(ZnTe) mode resonant replica.

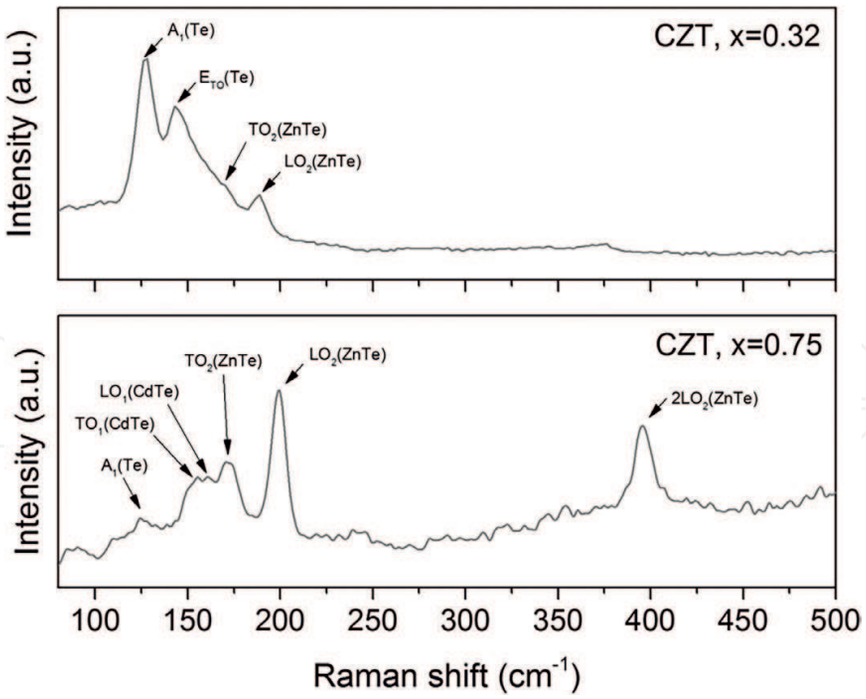

Figure 9. Raman spectra of CZT films measured during the impact of excitation irradiation of the wavelength 785 nm at room temperature (RT) [7].

http://dx.doi.org/10.5772/intechopen.72988

5. Conclusions

As a results of the complex study of structure, substructure, optical properties, and elemental composition of ZnO, CZTS, and CZT films obtained by pulsed spray pyrolysis technique dependent on the physical (chemical) and technological deposition conditions, it was determined that ZnO nanocrystalline films have an average grain size of D_C = 25–270 nm and their thickness was d = 0.8–1.2 μm, and were formed at T_s > 473 K. CZTS continuous films with optimal thickness of d = 1.3 μm were deposited at dispersed initial precursor volume V_s = 5 ml. It was found that ZnO and CZTS films were polycrystalline in nature, single-phase, and had hexagonal and tetragonal phases, respectively. CZTS samples had a kesterite structure.

It has been shown that in ZnO during the increasing of substrate temperature there is a tendency to the increasing of the CDS; however, in CZTS films, their CSD values were weakly depended on the dispersed solution volume.

Lattice parameters values in ZnO and CZTS films deposited at T_s = 623 K, V_s = 4 ml were well-correlated to the reference data that confirms their optimal stoichiometry and crystalline quality.

It has been estimated that during the increase of T_s the microdeformations level, microstresses, and dislocation density in ZnO films were decreased; in CZTS films, these parameters were weakly dependent on V_s.

It has been determined that during the increasing of substrate temperature to 623 K stoichiometry of ZnO layers was improved (γ_{ZnO} = 1.2). It has been shown that optimal for usage in SCs CZTS films, their stoichiometry ratios γ_{CZTS_1} = 0.8–0.9, γ_{CZTS_2} = 1.1–1.2, γ_{CZTS_3} = 0.7 were obtained at V_s = 3–4 ml.

Study of the optical characteristics of ZnO films allow to estimate the high values of transmission coefficient T = 60–80%. Measured E_g values of ZnO layers were determined in the range of 3.18–3.30 eV and had a complex dependence on T_s. During the increase of V_s, the values of E_g = 1.06–1.30 eV of CZTS layers were approximately approached to the reference data E_g = 1.5 eV. Raman spectra analysis of ZnO films confirmed the results of the XRD study, namely decreasing ε, σ, and ρ values during the increase of T_s. CZTS films' Raman spectra analysis has confirmed the single-phase nature of condensates. FTIR study indicated the absence of precursor impurities in ZnO films obtained at T_s > 573 K.

CZT film spectra (x = 0.32) had a mode LO_2(ZnTe). In these spectra, intensive peaks corresponded to A_1(Te) and E_{TO}(Te) tellure modes were also determined. CZT film spectra (x = 0.75) have a weak mode A_1(Te), peaks of LO_1(CdTe), TO_1(CdTe), TO_2(ZnTe), and LO_2(ZnTe) modes, and also LO_2(ZnTe) mode resonant replica.

The results of a research study of the ZnO, CZTS, and CZT thin films will be used for the development of the devices, primarily, in third generation high-efficiency thin-film solar cells.

Acknowledgements

This work was supported by the Ministry of the Education and Science of Ukraine (Grants numbers: 0116U002619, 0115U000665c, 0116U006813, and 0117U003929).

Author details

Oleksandr Dobrozhan, Denys Kurbatov*, Petro Danilchenko and Anatoliy Opanasyuk

*Address all correspondence to: dkurbatov@sumdu.edu.ua

Department of Electronics and Computer Technology, Sumy State University, Sumy, Ukraine

References

[1] Ozgur U, Alilov Y, Teke A. A comprehensive review of ZnO materials and devices. Applied Physics Reviews. 2005;**98**:041301. DOI: 10.1063/1.1992666

[2] Look D. Recent advances in ZnO materials and devices. Materials Science and Engineering B. 2001;**80**:383-387. DOI: 10.1016/S0921-5107(00)00604-8

[3] Kurbatova T, Khlyap H. State and economic prospects of developing potential of non-renewable and renewable energy resources in Ukraine (Review). Renewable and Sustainable Energy Reviews. 2015;**52**:217-226. DOI: 10.1016/j.rser.2015.07.093

[4] Kurbatova T, Khlyap H. GHG emissions and economic measures for low carbon growth in Ukraine. Carbon Management. 2015;**6**:7-17. DOI: 10.1080/17583004.2015.1065376

[5] Mahajan C, Takwale M. Intermittent spray pyrolytic growth of nanocrystalline and highly oriented transparent conducting ZnO thin films: Effect of solution spray rate. Journal of Alloys and Compounds. 2014;**584**:128-135. DOI: 10.1016/j.jallcom.2013.08.136

[6] Ito K, editor. Copper Zin Tin Sulfide-Based Thin Film Solar Cells. Chichester: Wiley; 2015. 440p. ISBN: 978-1-118-43787-2

[7] Kosyak V, Znamenshchykov Y, Cerskus A. Composition dependence of structural and optical properties of $Cd_{1-x}Zn_xTe$ thick films obtained by the close-spaced sublimation. Journal of Alloys and Compounds. 2016;**682**:543-551. DOI: 10.1016/j.jallcom.2016.05.065

[8] Prasada Rao T, Santhosh M, Safarulla K. Physical properties of ZnO thin films deposited at various substrate temperatures using spray pyrolysis. Physica B: Condensed Matter. 2010;**405**:2226-2231. DOI: 10.1016/j.physb.2010.02.016

[9] Shinde N, Deokate R, Lokhande C. Properties of spray pyrolysis deposited Cu_2ZnSnS_4 (CZTS) thin films. Journal of Analytical and Applied Pyrolysis. 2013;**100**:12-16. DOI: 10.1016/j.jaap.2012.10.018

[10] Gaikwad S, Tembhurkar Y, Dudhe C. Effect of substrate temperature on optical band gap and thickness of spray pyrolitically deposited $CdZnTe_2$ thin films. International Journal of Science and Research. 2017;**6**:1627-1634. DOI: 10.21275/ART20177528

[11] Gaikwad S, Tembhurkar Y, Dudhe C. Optical and electrical properties of spray pyrolitically deposited $CdZnTe_2$ thin films. International Journal of Pure and Applied Physics. 2017;**13**:231-240

[12] Arakelova E, Khachatryan A, Kteyan A. ZnO film deposition by DC magnetron sputtering: Effect of target configuration on the film properties. Thin Solid Films. 2016;**612**:407-413. DOI: 10.1016/j.tsf.2016.06.030

[13] Zhao Q, Hao R, Liu S. Fabrication and characterization of Cu_2ZnSnS_4 thin films by sputtering a single target at different temperature. Physica B: Condensed Matter. 2017;**523**:62-66. DOI: 10.1016/j.physb.2017.08.035

[14] Gao X, Zhu X, Sun H. Preparation and characterization of CdZnTe multilayer films by repeated RF magnetron sputtering. Journal of Materials Science: Materials in Electronics. 2017;**28**:4467-4474. DOI: 10.1007/s10854-016-6079-8

[15] Mooney J, Radding S. Spray pyrolysis processing. Annual Review of Materials Research. 1982;**12**:81-101. DOI: 10.1146/annurev.ms.12.080182.000501

[16] Tan S, Chen B, Sun X. Blueshift of optical band gap in ZnO thin films grown by metal-organic chemical-vapor deposition. Journal of Applied Physics. 2005;**98**:013505. DOI: 10.1063/1.1940137

[17] Riha S, Fredrick S, Sambur J. Photoelectrochemical characterization of nanocrystalline thin-film Cu_2ZnSnS_4 photocathodes. ACS Applied Materials and Interfaces. 2011; **3**:013505. DOI: 10.1021/am1008584

[18] Dobrozhan A, Opanasyuk A, Kolesnyk M. Substructural investigations, Raman, and FTIR spectroscopies of nanocrystalline ZnO films deposited by pulsed spray pyrolysis. Physica Status Solidi. 2015;**212**:2915-2921. DOI: 10.1002/pssa.201532324

[19] Dobrozhan O, Kurbatov D, Opanasyuk A. Influence of substrate temperature on the structural and optical properties of crystalline ZnO films obtained by pulsed spray pyrolysis. Surface and Interface Analysis. 2015;**47**:601-606. DOI: 10.1002/sia.5752

[20] Dobrozhan O, Loboda V, Ya Z. Structural and optical properties of Cu_2ZnSnS_4 films obtained by pulsed spray pyrolysis. Journal of Nano- and Electronic Physics. 2017; **9**:01028. DOI: 10.21272/jnep.9(1).01028

[21] Gorbik P, Dubrovin I, Filonenko M. Chemical method of obtaining the nanocrystalline texture ZnO films. Physics and Chemistry of Solid State. 2004;**5**:552-556

[22] Bacaksiz E, Aksu S, Yilmaz S. Structural, optical and electrical properties of Al-doped ZnO microrods prepared by spray pyrolysis. Thin Solid Films. 2010;**518**:4076-4080. DOI: 10.1016/j.tsf.2009.10.141

[23] Zaier A, Oum El az F, Lakfif F. Effects of the substrate temperature and solution molarity on the structural opto-electric properties of ZnO thin films deposited by spray pyrolysis. Materials Science in Semiconductor Processing. 2009;**12**:207-211

[24] Ayouchi R, Leinen D, Martin F. Preparation and characterization of transparent ZnO thin films obtained by spray pyrolysis. Thin Solid Films. 2003;**426**:68-77

[25] Ashour A, Kaid M, El-Sayed N. Physical properties of ZnO thin films deposited by spray pyrolysis technique. Applied Surface Science. 2006;**252**:7844-7848. DOI: 10.1016/j.apsusc.2005.09.048

[26] Riad A, Mahmoud S, Ibrahim A. Structural and DC electrical investigations of ZnO thin films prepared by spray pyrolysis technique. Physica B: Condensed Matter. 2001;**296**:319-325. DOI: 10.1016/S0921-4526(00)00571-8

[27] Shinde S, Patil G, Kajele D. Synthesis of ZnO nanorods by spray pyrolysis for H_2S gas sensor. Journal of Alloys and Compounds. 2012;**528**:109-114. DOI: 10.1016/j.jallcom.2012.03.020

[28] Moreno R, Ramirez E, Guzman G. Study of optical and structural properties of CZTS thin films grown by co-evaporation and spray pyrolysis. Journal of Physics Conference Series. 2016;**687**:012041. DOI: 10.1088/1742-6596/687/1/012041

[29] Nakayama N, Ito K. Sprayed films of stannite Cu_2ZnSnS_4. Applied Surface Science. 1996;**92**:171-175. DOI: 10.1016/0169-4332(95)00225-1

[30] Babu G, Kumar Y, Bhaskar P. Growth and characterization of co-evaporated Cu_2ZnSnS_4 thin films for photovoltaic applications. Journal of Physics D: Applied Physics. 2008;**41**:205305. DOI: 10.1088/0022-3727/41/20/205305

[31] Cui Y, Zuo S, Jiang J. Synthesis and characterization of co-electroplated Cu_2ZnSnS_4 thin films as potential photovoltaic material. Solar Energy Materials and Solar Cells. 2011;**95**:2136-2140. DOI: 10.1016/j.solmat.2011.03.013

[32] Paier J, Asahi R, Nagoya A. Cu_2ZnSnS_4 as a potential photovoltaic material: A hybrid Hartree-Fock density functional theory study. Physical Review B. 2009;**79**:115126. DOI: 10.1103/PhysRevB.79.115126

[33] Selected Powder Diffraction Data for Education and Training (Search Manual and Data Cards). Pennsylvania: International Center for Diffraction Data; 1998

[34] Rajeshmon V, Kartha C, Vijayakumar K. Role of precursor solution in controlling the opto-electronic properties of spray pyrolysed Cu_2ZnSnS_4 thin films. Solar Energy. 2012;**85**:249-255. DOI: 10.1016/j.solener.2010.12.005

[35] Opanasyuk A, Kurbatov D, Kosyak V. Characteristics of structure formation in zinc and cadmium chalcogenide films deposited on nonorienting substrates. Crystallography Reports. 2012;**57**:927-933

[36] Valdes M, Santoro G, Vazques M. Spray deposition of Cu_2ZnSnS_4 thin films. Journal of Alloys and Compounds. 2014;**585**:776-782. DOI: 10.1016/j.jallcom.2013.10.009

[37] Khalate S, Kate R, Kim J. Effect of deposition temperature on the properties of Cu_2ZnSnS_4 (CZTS) thin films. Superlattices and Microstructures. 2017;**103**:335-342. DOI: 10.1016/j.spmi.2017.02.003

[38] Ozutok F, Demirselcuk B, Sarica E. Study of ultrasonically sprayed ZnO films: Thermal annealing effect. Acta Physica Polonica A. 2012;**121**:53-55

[39] Kumar Y, Babu G, Bhaskar P. Preparation and characterization of spray-deposited Cu_2ZnSnS_4 thin films. Solar Energy Materials and Solar Cells. 2009;**93**:1230-1237. DOI: 10.1016/j.solmat.2009.01.011

[40] Touatia R, Ben Rabeh M, Kanzari M. Structural and optical properties of the new absorber Cu_2ZnSnS_4 thin films grown by vacuum evaporation method. Energy Procedia. 2014;**44**:44-51. DOI: 10.1016/j.egypro.2013.12.008

[41] Tanaka K, Moritake N, Uchiki H. Preparation of Cu_2ZnSnS_4 thin films by sulfurizing sol-gel deposited precursors. Solar Energy Materials and Solar Cells. 2007;**13**:1199-1201. DOI: 10.1016/j.solmat.2007.04.012

[42] Mitzi D, Gunawan O, Todorov T. The path towards a high-performance solution-processed kesterite solar cell. Solar Energy Materials and Solar Cells. 2011;**95**:1421-1436. DOI: 10.1016/j.solmat.2010.11.028

[43] Wong E, Searson P. ZnO quantum particle thin films fabricated by electrophoretic deposition. Applied Physics Letters. 1999;**74**:2939-2941. DOI: 10.1063/1.123972

[44] Ayouchi R, Martin F, Leinen D. Growth of pure ZnO thin films prepared by chemical spray pyrolysis on silicon. Journal of Crystal Growth. 2003;**247**:497-504. DOI: 10.1016/S0022-0248(02)01917-6

[45] Bendall J, Visimberga G, Szachowicz M. An investigation into the growth conditions and defect states of laminar ZnO nanostructures. Journal of Materials Chemistry. 2008;**18**:5259-5266. DOI: 10.1039/B812867G

[46] Shinde S, Bhosale C, Rajpure K. Structural, optical, electrical and thermal properties of zinc oxide thin films by chemical spray pyrolysis. Journal of Molecular Structure. 2012;**1021**:123-129. DOI: 10.1016/j.molstruc.2012.04.045

[47] Bedia A, Bedia F, Aillerie A. Optical, electrical and structural properties of nano-pyramidal ZnO films grown on glass substrate by spray pyrolysis technique. Optical Materials. 2012;**36**:1123-1130. DOI: 10.1016/j.optmat.2014.02.012

[48] Karber E, Raadik T, Dedova T. Photoluminescence of spray pyrolysis deposited ZnO nanorods. Nanoscale Research Letters. 2011;**6**:359. DOI: 10.1186/1556-276X-6-359

[49] Li Z, Hu Z, Liu F. Lateral growth and optical properties of ZnO microcrystal on sapphire substrate. Optical Materials. 2012;**34**:1908-1912. DOI: 10.1016/j.optmat.2012.05.033

[50] Khan Z, Khan M, Zulfequar M. Optical and structural properties of ZnO thin films fabricated by sol-gel method. Materials Sciences and Applications. 2011;**52**:340-345. DOI: 10.4236/msa.2011.25044

[51] Kishore Kumar Y, Uday Bhaskar P, Suresh Babu G. Effect of copper salt and thiourea concentrations on the formation of Cu_2ZnSnS_4 thin films by spray pyrolysis. Physica Status Solidi. 2010;**207**:149-156. DOI: 10.1002/pssa.200925194

[52] Fernandes P, Salome P, da Cunha A. Study of polycrystalline Cu_2ZnSnS_4 films by Raman scattering. Journal of Alloys and Compounds. 2011;**509**:7600-7606. DOI: 10.1016/j.jallcom.2011.04.097

[53] Patel M, Mukhopadhyay I, Ray A. Structural, optical and electrical properties of spray-deposited CZTS thin films under a non-equilibrium growth condition. Journal of Physics D. 2012;**45**:445103. DOI: 10.1088/0022-3727/45/44/445103

[54] Fernandes P, Salome P, da Cunha A. Growth and Raman scattering characterization of Cu_2ZnSnS_4 thin films. Thin Solid Films. 2009;**517**:2519-2523. DOI: 10.1016/j.tsf.2008.11.031

[55] Fontane X, Calvo-Barrio L, Izquierdo-Roca V. In-depth resolved Raman scattering analysis for the identification of secondary phases: Characterization of Cu_2ZnSnS_4 layers for solar cell applications. Applied Physics Letters. 2011;**98**:181905. DOI: 10.1063/1.3587614

[56] Dumcenco D, Huang Y. The vibrational properties study of kesterite Cu_2ZnSnS_4 single crystals by using polarization dependent Raman spectroscopy. Optical Materials. 2013;**35**:419-425. DOI: 10.1016/j.optmat.2012.09.031

[57] Kodigala S. Thin film solar cells from earth abundant materials: Growth and characterization of $Cu_2(Zn,Sn)(S,Se)_4$ thin films and their solar cells. London: Newnes; 2013. 190p. ISBN: 9780123944290